2011 American Control Conference
on O'Farrell Street, San Francisco, CA, USA
June 29 - July 01, 2011

# A Method for Reducing Piezoelectric Non-Linearity in Scanning Probe Microscope Images

Andrew J. Fleming†
School of Electrical Eng. and Computer Science
The University of Newcastle
NSW 2300, Australia
andrew.fleming@newcastle.edu.au

***Abstract*— This paper describes a new technique for reducing the piezoelectric hysteresis in SPM images. Imaging modes such as constant-force AFM require a piezoelectric actuator to vary the probe-sample distance. In such modes, the topography of the sample is reconstructed from the voltage applied to the vertical piezoelectric actuator. However, piezoelectric actuators exhibit significant hysteresis which can produce up to 14% uncertainty in the reproduced topography. To combat this problem, the recent generation of commercial AFM's use capacitive or inductive position sensors to eliminate hysteresis; however, these sensors can be difficult to incorporate into the scanning head and also increase the imaging noise. In this work, an alternative technique is proposed that avoids the use of a vertical position sensor. Instead, a charge amplifier is utilized to linearize the vertical piezoelectric actuator and eliminate imaging hysteresis. Experimental results demonstrate a reduction in non-linearity from from 14% to 0.65%, which is visibly undetectable.**

## I. Introduction

Scanning Probe Microscopes (SPMs) record localized physical interactions between a probe and sample as a function of position. A diverse range of techniques and probes have become available to image properties such as topography, electrical and mechanical forces, chemical bonding and biological interactions [1]–[5].

Many popular modes of scanning probe microscopy require a vertical feedback system to regulate the probe-sample interaction. Examples include constant-current scanning tunneling microscopy and constant-force atomic force microscopy. These techniques ensure that the probe-sample interaction is kept constant by varying the probe or sample height. Rather than recording the cantilever deflection, which is a highly non-linear function of topography, the image is reproduced from the control voltage applied to the vertical actuator. It is assumed that the control voltage is directly proportional to position and hence topography.

Due to their high speed, compact size and essentially infinite resolution, piezoelectric actuators are used almost exclusively in scanning probe microscopes. SPM scanners and vertical positioners are usually constructed from either piezoelectric tube actuators [6], [7] or faster piezoelectric stack actuators [8]. Although scanners constructed from piezoelectric actuators have extremely high resolution, the overall accuracy is limited by creep and hysteresis [9]. For example, the positioning error due to hysteresis in a piezoelectric tube actuator has been reported to be $\pm 9.7\%$ of the scan-range [10]. This implies a maximum positioning error of almost 20% between the forward and backward scanning paths.

To avoid imaging artifacts, SPM's require some form of compensation for positioning non-linearity. Methods to accomplish this, including feedback and feedforward control, have been recently surveyed [9], [11], [12]. However, these methods are aimed at reducing lateral positioning error and do not consider vertical axis non-linearity.

It is generally accepted that piezoelectric non-linearity can be neglected in the vertical axis since hysteresis is voltage dependent and the sample features will be small compared to the full-scale range of the scanner. However, this can be a poor assumption, particularly when the sample substrate is sloping which requires large excursions from the vertical positioner. It is also not uncommon for sample features to exceed 10% of the full-scale range, especially in microscopes designed for high-speed [8], [13]–[17]. Even at 5% of the full-scale range, hysteresis has been shown to result in up to $\pm 2\%$ error, and $\pm 4.9\%$ error at 20% of the full-scale range [10]. Thus, it should not be neglected if quantitative topographical information is desired.

Recently, the presence of vertical non-linearity has been addressed by metrological SPMs [18]. Rather than simply recording the applied actuator voltage, metrological SPMs contain a position sensor to measure the vertical displacement directly. As the actuator non-linearity is bypassed, the recorded image is a quantitative reproduction of the sample topography.

The disadvantage of metrological SPMs is inherent in their design, they require a linear position sensor capable of large range, wide-bandwidth and high resolution. This requirement can significantly increase the scanner complexity and dramatically increases the cost. Furthermore, typical position sensors are much noisier than the control voltage applied to a vertical actuator. For example, the peak-to-peak noise of the laser interferometer used in the aforementioned SPM is 4 nm [18].

The most recent generation of commercial AFM's use a

978-1-4577-0079-8/11/$26.00 ©2011 AACC

capacitive or inductive position sensor to directly measure the vertical topography. These sensors have a range of around 10 $\mu$m, a uncorrected linearity of around 1%, and a typical noise density of 3 pm/$\sqrt{\text{Hz}}$. In this work the spectral density is assumed to be double-sided, that is, it is defined by

$$S_{\mathcal{X}}(f) = \int_{-\infty}^{\infty} R_{\mathcal{X}}(\tau) e^{-j2\pi f \tau} \, d\tau, \tag{1}$$

where $R_{\mathcal{X}}(\tau)$ is the autocorrelation. If the noise is assumed to be Guassian distributed with a bandlimited constant spectral density, the peak-to-peak noise is approximately

$$\text{Peak-to-Peak Noise} = 6 \times \text{Noise Density} \times \sqrt{2 \times \text{Bandwidth}}. \tag{2}$$

Hence, a typical position sensor with a bandwidth of 1 kHz exhibits a peak-to-peak noise of approximately 800 pm. This is insufficient for atomic resolution; however, if the bandwidth is reduced to 10 Hz, the noise reduces to 80 pm and atomic resolution can be obtained.

A penalty of reducing the position sensor bandwidth is lower imaging speed. Based on the assumptions of triangular scanning and ten features per line, the position sensor bandwidth needs to be approximately two-hundred times the scan-rate for 'sharp' samples, and twenty times the scan-rate for 'smooth' samples. Hence, if the position sensor bandwidth is limited to 10 Hz, the scan-rate must be limited to 0.5 Hz for smooth samples and 0.05 Hz for sharp samples. A scan-rate of 0.05 Hz would require eight minutes for a 100×100 resolution image, which is prohibitively slow.

Due to the noise generated by position sensors, they are rarely used in high resolution imaging. Instead, the topography is acquired in the traditional manner from the applied actuator voltage, albeit at the expense of poor linearity as discussed above. To appreciate the improvement in noise performance, consider a standard 200 V amplifier with a 1-kHz bandwidth and a peak-to-peak noise of 1 mV (e.g. the PiezoDrive PDL200 amplifier). Using a piezoelectric actuator with a range of 10 um, the sensitivity is 50 nm/V which implies a peak-to-peak noise of only 50 pm. This figure is only 6% of the position sensor noise and demonstrates why the applied actuator voltage is preferred for atomic scale imaging.

In this work a new approach is demonstrated for obtaining quantitative topographical information from a standard SPM. Rather than the use of a position sensor or hysteresis model, the vertical axis voltage amplifier is simply replaced by a charge drive. As piezoelectric actuators respond more linearly to charge or current rather than voltage [19], hysteresis is substantially reduced. In Section III the hysteresis of a piezoelectric stack actuator is reduced from 14.3% of the full-scale range to 0.65%. In Section IV this reduction is demonstrated to dramatically improve the linearity and reproducibility of the recorded topography. This technique can be easily retrofitted to any commercial SPM and avoids the problem of actuator nonlinearity without the addition of position sensor noise.

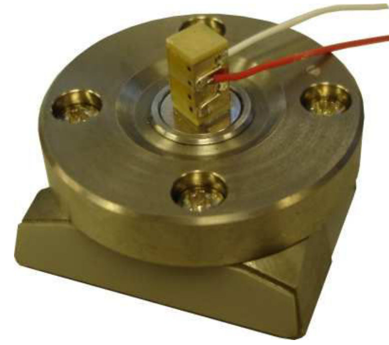

Fig. 1. The vertical positioner is a 10-mm piezoelectric stack actuator (Noliac SCMAP07) bonded to a standard base-plate. The sample holder is affixed to the top of the stack.

This paper proceeds in the following section with a description of the experimental setup.

## II. Experimental Setup

The proposed techniques are demonstrated on an NT-MDT Ntegra SPM arranged in a scan-by-probe configuration. The scanner is an NT-MDT Sm8122cl piezoelectric tube scanner with 100-$\mu$m lateral range and 10-$\mu$m vertical range. Since the scanner resonance frequency is only 680 Hz [20], the vertical positioning function is replaced by a high-speed piezoelectric stack actuator as pictured in Figure 1. The actuator is a 10-mm long Noliac SCMAP07 stack actuator epoxy-bonded to a standard microscope base. The sample holder is glued directly onto the top of the actuator. A full-scale extension of 10.5 $\mu$m is developed from a 200-V applied voltage.

The use of a separate vertical positioning stage eliminates the presence of low-frequency lateral resonance modes in the vertical feedback loop. This approach has been reported to increase the z-axis bandwidth by more than an order of magnitude [17], [20], [21].

The maximum vertical feedback bandwidth has previously been shown to be [17],

$$\text{Maximum Bandwidth} = \frac{\text{Resonance Frequency}}{\text{Peak Amplitude}}, \tag{3}$$

where the peak amplitude is the magnitude at the resonance frequency divided by the DC-Gain.

The first resonance frequency of the vertical stage pictured in Figure 1 occurs at 20.3 kHz and the peak amplitude is 2.6 (or 8.3 dB). This allows a maximum vertical feedback bandwidth of 7.8 kHz, which is 65 times faster than the standard maximum bandwidth of 120 Hz [17].

The operation of the vertical feedback loop during constant-force contact-mode AFM is illustrated in Figure 2. The controller $C(s)$ maintains a constant probe-sample interaction while the image profile is obtained from the

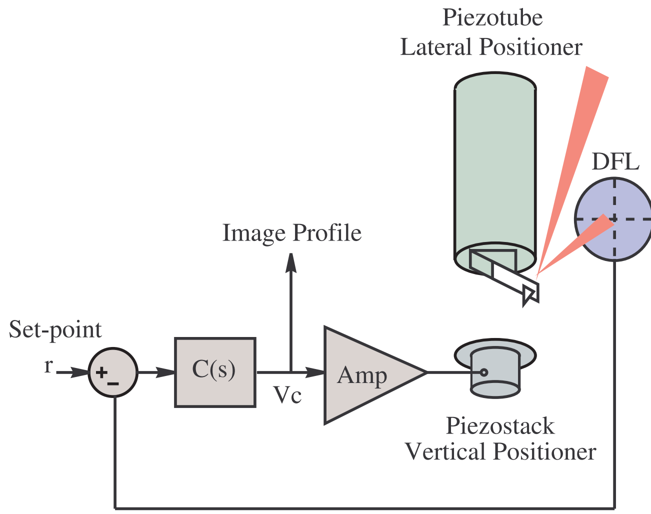


Fig. 2. Schematic diagram of the vertical feedback loop operating in constant-force contact-mode AFM. The image profile is the voltage applied to the amplifier.

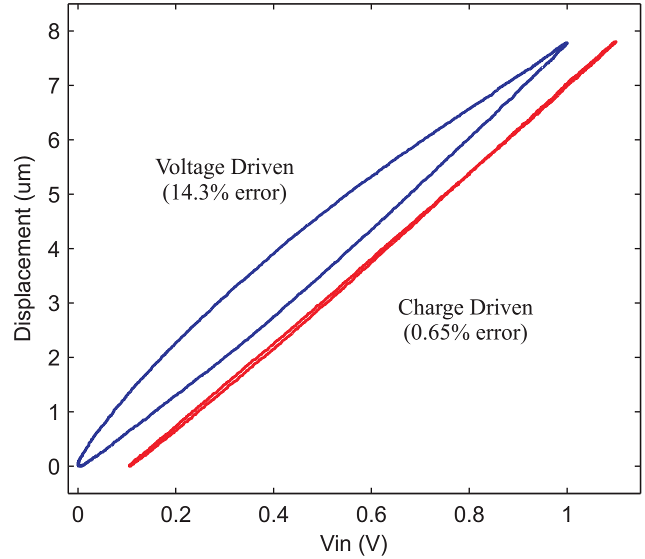


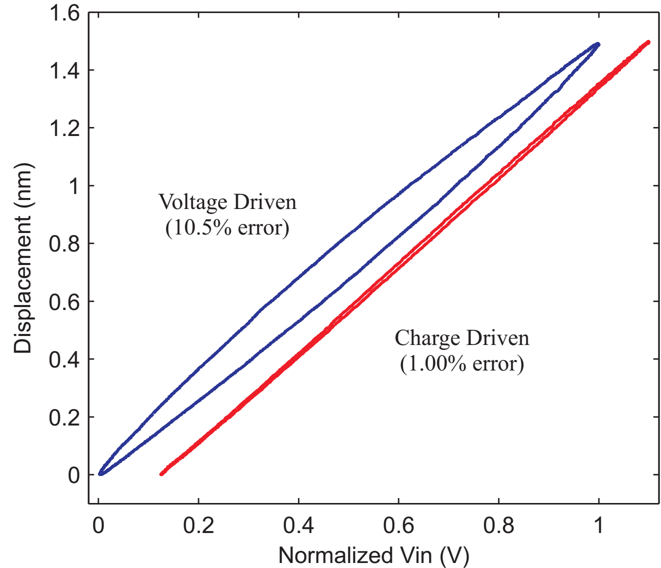


Fig. 3. A comparison of hysteresis exhibited by the voltage- and charge-driven piezoelectric positioner shown in Figure 1. The input signal was a 100-Hz sine-wave with a peak-to-peak voltage of 150 V in (A) and 30 V in (B). (The charge-driven results are offset for clarity)

voltage applied to the vertical axis amplifier. This mode of operation is similar to many forms of SPM where the probe-sample interaction is controlled. Different operating modes use different feedback variables. For example, in constant-force contact-mode AFM, the feedback variable is cantilever deflection. In constant-current STM, the feedback variable is tunneling current. Other feedback variables include the cantilever oscillation magnitude in tapping-mode AFM and the fiber oscillation magnitude in scanning near-field optical microscopy.

The linearity of the vertical axis positioner is examined in the following section.

## III. Linearization of the Vertical Axis

In Figure 2, the vertical feedback loop of an AFM is shown while operating in constant-force contact-mode. To derive the image profile from the control voltage $V_c$, the sensitivity of the amplifier $K_a$ and positioner $K_p$ must be known. For the setup described above, the amplifier gain is $K_a = 20$ V/V, and the positioner sensitivity is $K_p = 53$ nm/V. The image profile is thus $V_c(x, y) \times K_a K_p$ or $V_c(x, y) \times 1.06$ $\mu$m.

Clearly the image profile relies on a proportional relationship between the applied voltage and resulting displacement. The validity of this assumption was tested by applying a 10-Hz 150-V sine-wave to the actuator then recording the displacement with a Polytec-PI MSV400 Laser Vibrometer. The results are plotted in Figure 3(a). The maximum difference in position between two points with the same applied voltage was 1.1 $\mu$m or 14.3% of the range. A second experiment was conducted to examine the non-linearity when operating at only 30 V or 15% of the full-scale range. Although reduced, the error due to hysteresis was still 157 nm or 10.5% of the range. From these results, it can be concluded that a quantitative topography cannot be obtained directly from the control voltage $V_c$. Similar magnitudes of non-linearity have been reported using piezoelectric tubes rather than stack actuators [10].

As discussed in the introduction, metrological SPMs use a position sensor to bypass the actuator non-linearity. In the present work, rather than bypassing the actuator, the actuator is linearized by applying charge instead of voltage.

It has been known since the 80's that piezoelectric transducers respond more linearly to current or charge rather than voltage [19]. However, practical problems with drift and the floating nature of the load were only recently solved [22],

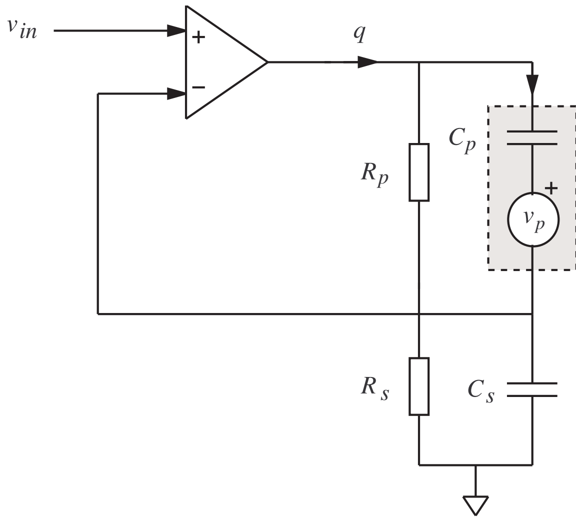


Fig. 4. Simplified schematic diagram of a charge drive. The piezoelectric load is shaded in gray.

[23]. Since then, charge drives have been demonstrated to reduce the hysteresis of SPM tube scanners by up to 93% [10]. This corresponds to a maximum non-linearity of less than 1% that effectively eliminates the need for feedback or feedforward control in dynamic applications.

A simplified schematic diagram of the charge drive used in this work is shown in Figure 4. Since the piezoelectric stack actuator does not require a grounded electrode, the floating-load circuit [22] was used instead of the grounded-load arrangement [23]. In Figure 4, the piezoelectric load is modeled as a capacitor $C_p$ and voltage source $v_p$. The high-gain feedback loop works to equate the applied reference voltage $v_{in}$, to the voltage across a sensing capacitor $C_s$. Neglecting the resistances $R_p$ and $R_s$, the charge $q$ is

$$q = V_{in} C_s. \tag{4}$$

That is, the gain is $C_s$ Coulombs/V. When connected to a capacitive load, the equivalent voltage gain is $C_s/C_p$. As discussed previously [24], the existence of $R_p$ and $R_s$ introduces error at low-frequencies. However, by ensuring that the ratio of resistances is equal to the inverse ratio of capacitances, low-frequency error can be eliminated. That is, by setting

$$\frac{R_p}{R_s} = \frac{C_s}{C_p}, \tag{5}$$

the amplifier has a constant gain of $C_s$ Coulombs/V over all frequencies.

As the actuator capacitance is $C_p = 330$ nF, a sensing capacitance of 22 $\mu$F was chosen to provide a voltage gain of 66. To maintain this voltage gain at DC, the parallel resistances were chosen to be $R_p = 6.6$ MΩ and $R_s = 100$ kΩ. This circuit was implemented by a PiezoDrive PDQ200 charge amplifier.

The response of the charge-driven piezoelectric actuator is plotted in Figure 3. The maximum non-linearity with a 150-V excitation is 51 nm or 0.65% of the range. With a 30-V excitation, the maximum non-linearity is 15 nm or 1% of the range. These results are summarized in Table I. Although the maximum residual hysteresis of 1% is not comparable to the linearity of a laser interferometer, this magnitude of error is sufficient for many applications that require quantitative topographical information.

TABLE I

THE MAXIMUM ERROR DUE TO HYSTERESIS OF THE VOLTAGE- AND CHARGE-DRIVEN PIEZOELECTRIC ACTUATOR.

| Range | Absolute Error | | % Error | | Reduction |
|---|---|---|---|---|---|
| | Voltage | Charge | Voltage | Charge | |
| 7.8$\mu$m | 1.1$\mu$m | 51nm | 14.3% | 0.65% | 95% |
| 1.5$\mu$m | 157nm | 15nm | 10.5% | 1.00% | 90% |

In addition to the improvement in linearity, charge drives have a number of advantages over physical position sensors. First, they are low-cost and are easily retrofitted to any SPM without mechanical modifications. Second, the random noise produced by a charge drive is similar to that of a voltage amplifier [10], which, as discussed in the introduction, is significantly less than a physical position sensor.

The random noise generated by a charge drive is similar to a voltage amplifier since the topology of both circuits is almost identical. In both cases, the amplifier's input noise voltage is the dominant process since this is multiplied by the gain of the circuit. Since charge amplifiers have a high-impedance output, they are more susceptible to interference than voltage amplifiers. If the output is not appropriately shielded, additional noise can result.

With the load capacitance attached, the output noise voltage of the PDQ200 charge amplifier was measured to be 1.5 mV RMS. This was measured by a Fluke 289 multimeter with a 100-kHz measurement bandwidth. The same circuit configured as a voltage amplifier generated an output voltage noise of 1.2 mV RMS, hence there is little noise penalty when using a charge drive.

Another consideration with charge amplifiers is the bandwidth. As the circuit topology of a charge amplifier is similar to a voltage amplifier, the bandwidth is also similar. However, for effective rejection of the disturbance caused by hysteresis, the internal loop-gain needs to be greater than approximately 20 dB. This occurs at frequencies lesser than one-tenth of the bandwidth.

The bandwidth of the PDQ200 charge amplifier was measured to be 51 kHz. This means that significant hysteresis rejection only occurs at frequencies below 5 kHz. This is not a significant disadvantage as all amplifiers have a bandwidth of at least ten times the maximum signal frequency so that phase lag and magnitude shift can be avoided. In this case it is not possible to experimentally measure the hysteresis response over a wide frequency range due to the current limit of the amplifier and self-heating of the actuator.

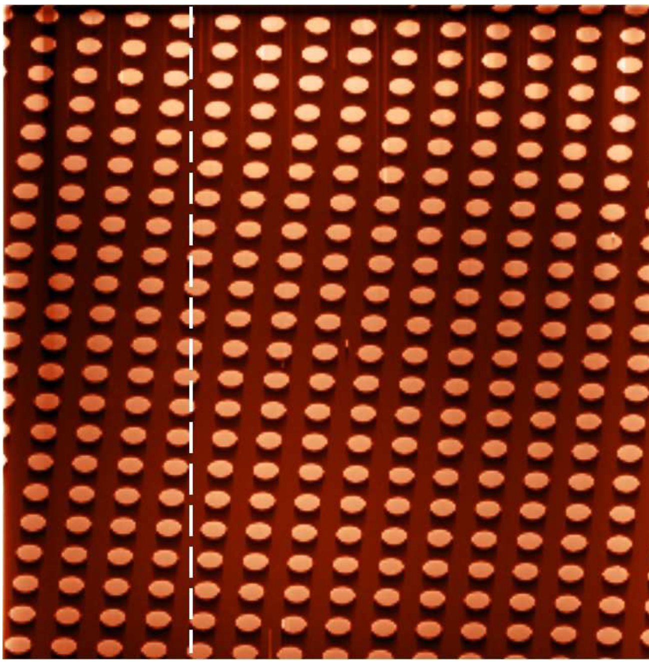

Fig. 5. The topography of a BudgetSensors HS-100MG calibration grating imaged in constant-force contact-mode. The scan area is 100 $\mu$m and the feature height is 100 nm. The dashed line indicates the location of the single profile line plotted in Figure 6.

## IV. Imaging Performance

In this section we compare the topographic profiles of an AFM image acquired using a voltage- and charge-driven vertical actuator. The sample under consideration is a BudgetSensors HS-100MG calibration grating. A constant-force contact-mode AFM image of the sample (using a voltage amplifier) is shown in Figure 5. The sample slope was removed by subtracting a second-order plane.

Also shown in Figure 5 is a dashed line that illustrates the location of a single profile line. When using a voltage-driven vertical actuator, the raw profile is plotted in Figure 6(a). In this plot, the piezoelectric hysteresis is observed to add significant curvature to the profile and introduce a large discrepancy between the forward and backwards scan paths. After replacing the voltage amplifier with a charge drive, the same image line is plotted in Figure 6(b). With the hysteresis reduced to a negligible level, the linearity and reproducibility are greatly improved.

## V. Conclusions

In this work, piezoelectric hysteresis was demonstrated to cause an uncertainty of up to 14.3% in the topography of an SPM image. Even small vertical excursions resulted in a 10.5% error due to hysteresis. This magnitude of error precludes the acquisition of quantitative toppgraphical information from an SPM without a position sensor or other compensation for vertical non-linearity.

To reduce the image uncertainties, a charge drive was proposed to linearize the vertical piezoelectric actuator. In experiments, the error due to hysteresis was reduced by at least 90%, to 1% of the range. This was sufficient to eliminate visible artefacts in a constant-force contact-mode AFM profile.

Although displacement sensors such as laser interferometers can provide better linearity than a charge-driven piezoelectric actuator, they also require significant mechanical modifications, are costly, and may be too noisy to achieve atomic resolution. Charge amplifiers are a simple, high-performance alternative for conventional SPMs when topographical uncertainties of 1% can be tolerated.

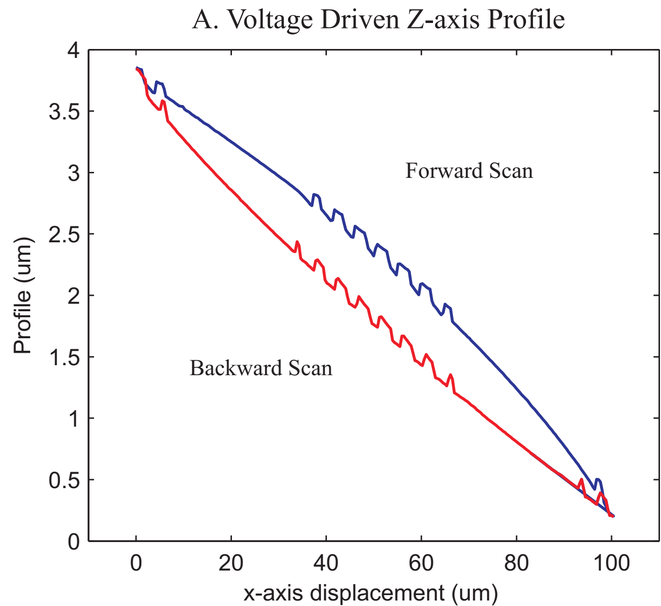


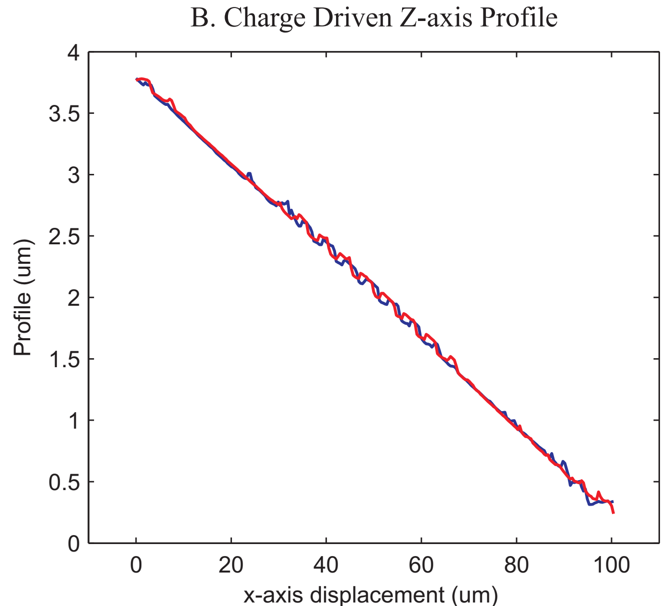


Fig. 6. The profile of a single image line acquired using a voltage-driven (A) and charge-driven (B) vertical positioner.

## Acknowledgements

This research was supported by an Australian Research Council Discovery Project (DP0986319). Experiments were carried out at the Laboratory for Dynamics and Control of Nanosystems at the University of Newcastle.


## References


[1] M. J. Brukman and D. A. Bonnell, "Probing physical properties at the nanoscale," *Physics Today*, vol. 61, no. 6, pp. 36–42, June 2008.

[2] Y. F. Dufrêne, "Towards nanomicrobiology using atomic force microscopy," *Nature Reviews Microbiology*, vol. 6, pp. 674–680, September 2008.

[3] D. Bonnell, Ed., *Scanning probe microscopy and spectroscopy. Theory, Techniques, and Applications. Second Edition.* Hoboken, NJ: Wiley-VCH, 2001.

[4] E. Meyer, H. J. Hug, and R. Bennewitz, *Scanning probe microscopy. The lab on a tip*. Heidelberg, Germany: Springer-Verlag, 2004.

[5] B. Bhushan, Ed., *The handbook of nanotechnology*. Springer-Verlag, 2004.

[6] G. Binnig and D. P. E. Smith, "Single-tube three-dimensional scanner for scanning tunneling microscopy," *Review of Scientific Instruments*, vol. 57, no. 8, pp. 1688–1689, August 1986.

[7] S. O. R. Moheimani, "Accurate and fast nanopositioning with piezoelectric tube scanners: Emerging trends and future challenges," *Review of Scientific Instruments*, vol. 79, no. 7, pp. 071 101(1–11), July 2008.

[8] G. E. Fantner, G. Schitter, J. H. Kindt, T. Ivanov, K. Ivanova, R. Patel, N. Holten-Andersen, J. Adams, P. J. Thurner, I. W. Rangelow, and P. K. Hansma, "Components for high speed atomic force microscopy," *Ultramicroscopy*, vol. 106, no. 2-3, pp. 881–887, June-July 2006.

[9] S. Devasia, E. Eleftheriou, and S. O. R. Moheimani, "A survey of control issues in nanopositioning," *IEEE Transactions on Control Systems Technology*, vol. 15, no. 5, pp. 802–823, September 2007.

[10] A. J. Fleming and K. K. Leang, "Charge drives for scanning probe microscope positioning stages," *Ultramicroscopy*, vol. 108, no. 12, pp. 1551–1557, November 2008.

[11] J. A. Butterworth, L. Y. Pao, and D. Y. Abramovitch, "A comparison of control architectures for atomic force microscopes," *Asian Journal of Control*, vol. 11, no. 2, pp. 175–181, March 2009.

[12] G. M. Clayton, S. Tien, K. K. Leang, Q. Zou, and S. Devasia, "A review of feedforward control approaches in nanopositioning for high-speed SPM," *Journal of Dynamic Systems, Measurement, and Control*, vol. 131, pp. 061 101(1–19), November 2009.

[13] T. Ando, N. Kodera, T. Uchihashi, A. Miyagi, R. Nakakita, H. Yamashita, and K. Matada, "High-speed atomic force microscopy for capturing dynamic behavior of protein molecules at work," *e-Journal of Surface Science and Nanotechnology*, vol. 3, pp. 384–392, December 2005.

[14] A. D. L. Humphris, M. J. Miles, and J. K. Hobbs, "A mechanical microscope: high-speed atomic force microscopy," *Applied Physics Letters*, vol. 86, pp. 034 106(1–3), 2005.

[15] M. J. Rost, L. Crama, P. Schakel, E. van Tol, G. B. E. M. van Velzen-Williams, C. F. Overgauw, H. ter Horst, H. Dekker, B. Okhuijsen, M. Seynen, A. Vijftigschild, P. Han, A. J. Katan, K. Schoots, R. Schumm, W. van Loo, T. H. Oosterkamp, and J. W. M. Frenken, "Scanning probe microscopes go video rate and beyond," *Review of Scientific Instruments*, vol. 76, no. 5, pp. 053 710(1–9), April 2005.

[16] L. M. Picco, L. Bozec, A. Ulcinas, D. J. Engledew, M. Antognozzi, M. Horton, and M. J. Miles, "Breaking the speed limit with atomic force microscopy," *Nanotechnology*, vol. 18, no. 4, pp. 044 030(1–4), January 2007.

[17] A. J. Fleming, B. J. Kenton, and K. K. Leang, "Bridging the gap between conventional and video-speed scanning probe microscopes," *Ultramicroscopy*, vol. 110, no. 9, pp. 1205–1214, August 2010.

[18] R. Merry, M. Uyanik, R. van de Molengraft, R. Koops, M. van Veghel, and M. Steinbuch, "Identification, control and hysteresis compensation of a 3 DOF metrological AFM," *Asian Journal of Control*, vol. 11, no. 2, pp. 130–143, March 2009.

[19] C. V. Newcomb and I. Flinn, "Improving the linearity of piezoelectric ceramic actuators," *IEE Electronics Letters*, vol. 18, no. 11, pp. 442–443, May 1982.

[20] A. J. Fleming and K. K. Leang, "Integrated strain and force feedback for high performance control of piezoelectric actuators," *Sensors and Actuators A*, vol. 161, no. 1-2, pp. 256–265, June 2010.

[21] G. Schitter, "Improving the speed of AFM by mechatronic design and modern control methods," *Technisches Messen*, vol. 76, no. 5, pp. 266–273, May 2009.

[22] K. A. Yi and R. J. Veillette, "A charge controller for linear operation of a piezoelectric stack actuator," *IEEE Transactions on Control Systems Technology*, vol. 13, no. 4, pp. 517–526, July 2005.

[23] A. J. Fleming and S. O. R. Moheimani, "A grounded load charge amplifier for reducing hysteresis in piezoelectric tube scanners," *Review of Scientific Instruments*, vol. 76, no. 7, pp. 073 707(1–5), July 2005.

[24] ——, "Sensorless vibration suppression and scan compensation for piezoelectric tube nanopositioners," *IEEE Transactions on Control Systems Technology*, vol. 14, no. 1, pp. 33–44, January 2006.